

Article

Diagenetic Evolution and Petrophysical Characteristics of Paleogene Sandstone Reservoirs in the Southwest Baiyun Sag, Northern South China Sea

Guanyu Zhang ^{1,2}, Qiang Fu ^{1,2,*}, Guangrong Peng ^{3,4}, Xudong Wang ^{3,4}, Lili Zhang ^{3,4}, Xuhong Xiang ^{3,4} and Zhiwei Zhu ^{1,2}

¹ State Key Laboratory of Marine Geology, Tongji University, Shanghai 200092, China; 2010868@tongji.edu.cn (G.Z.)

² Center for Marine Resources, Tongji University, Shanghai 200092, China

³ CNOOC Ltd.-Shenzhen, Shenzhen 518054, China; xiangxh@cnooc.com.cn (X.X.)

⁴ CNOOC Deepwater Development Ltd., Shenzhen 518054, China

* Correspondence: fuqiang@tongji.edu.cn

Abstract: In addressing the critical need to understand the geological and diagenetic factors affecting Paleogene sandstone reservoirs in the Baiyun Sag—a region vital for oil and gas exploration—this study delves into the Paleogene Zhuhai and Enping formations. Advanced methodologies, including petrographic thin-section analysis, scanning electron microscopy, wavelet analysis, and carbon and oxygen isotope analysis, were employed to evaluate their petrological characteristics, pore structures, physical properties, and key diagenetic processes. The results indicate that the Zhuhai Formation is primarily composed of feldspathic quartz sandstones with prevalent intergranular dissolution pores, while the Enping Formation consists mainly of feldspathic sandstones with intragranular solution pores. The diagenetic temperatures across both formations ranged from 42.6 to 116.3 °C. The studied reservoirs have experienced porosity alterations due to mechanical compaction (23.07% reduction), carbonate cementation (9.02% reduction), and dissolution (5.09% enhancement). Notably, feldspar dissolution emerged as a significant contributor to high-quality reservoirs, particularly in the upper Enping Formation. These findings offer invaluable insights into the diagenetic evolution of sandstone reservoirs in the Baiyun Sag and hold significant implications for guiding future oil and gas exploration efforts in the region.

Keywords: baiyun sag; paleogene; diagenesis; diagenetic evolution



Citation: Zhang, G.; Fu, Q.; Peng, G.; Wang, X.; Zhang, L.; Xiang, X.; Zhu, Z. Diagenetic Evolution and Petrophysical Characteristics of Paleogene Sandstone Reservoirs in the Southwest Baiyun Sag, Northern South China Sea. *Minerals* **2023**, *13*, 1265. <https://doi.org/10.3390/min13101265>

Academic Editor: Luca Aldega

Received: 1 August 2023

Revised: 15 September 2023

Accepted: 25 September 2023

Published: 28 September 2023



Copyright: © 2023 by the authors. Licensee MDPI, Basel, Switzerland. This article is an open access article distributed under the terms and conditions of the Creative Commons Attribution (CC BY) license (<https://creativecommons.org/licenses/by/4.0/>).

1. Introduction

The Baiyun Sag, located in the Zhu II Depression of the Pearl River Mouth Basin, represents the largest and deepest sag within the basin. Its water depth ranges from 200 m to 2800 m, covering both shallow and deep-water areas [1,2]. This depression holds enormous unexplored resource potential, with the mid-depth Enping Formation's lithologic stratigraphic traps being crucial for exploration [3–5]. In the middle and deep layers of the Zhuhai Formation and below (depth greater than 3500 m), overpressure and high temperatures create a favorable “sweet spot” reservoir area for large-scale oil and gas exploration [6–9].

The current research area lies in the southwest of the Baiyun Sag, where only a few offshore wells have been drilled. More than half of the proven natural gas reserves are still locked in low-producing gas reservoirs. To enhance oil and gas exploration in the Baiyun Sag, it is essential to identify high-quality reservoirs despite overall poor reservoir physical properties. Scientists have conducted extensive research on the characteristics of mid-deep reservoirs and key controlling factors of high-quality reservoirs in the area. The upper part of the Enping Formation exhibits relatively good porosity and permeability, while the lower

part shows poorer physical reservoir conditions [10–13]. The diagenesis of the Enping Formation plays a crucial role in affecting the reservoir's properties [14,15]. Secondary porosity formed by mineral dissolution in the Paleogene reservoirs of the Pearl River Mouth Basin effectively improves reservoir storage capacity and fluid flow [16,17]. Exploration efforts should focus on potential high-quality reservoirs with developed secondary porosity in the middle and deep reservoirs of the Baiyun Sag [18–20].

However, previous studies have primarily focused on identifying the influence of secondary porosity formed by dissolution on the reservoir, without clearly indicating the relationship between diagenetic effects, such as Paleogene cementation and compaction in the southwest Baiyun Sag, and their impact on reservoir properties. The specific influence of diagenetic evolution on the physical properties of sandstone reservoirs in the region remains unclear. Building upon previous research, this study aims to comprehensively investigate the diagenesis, diagenetic stages, and pore evolution of Paleogene sandstone reservoirs in the southwest Baiyun Sag, utilizing existing drilling data and employing various analytical and testing methods. The analysis will clarify the genesis of different types of diagenetic minerals in the Paleogene sandstone reservoirs and their influence on pore development, providing a crucial geological basis for understanding the Paleogene reservoirs in the region and guiding future exploration efforts.

2. Geological Setting

2.1. Basin Evolution

The Baiyun Sag is situated in the Zhu II Depression, within the Pearl River Mouth Basin. It has an overall strike near the northeast, covering an area of more than 20,000 km², and a water depth ranging from 200 m to 2800 m. The main body of the Baiyun Sag is located in the deep water of the continental slope on the northern continental margin of the South China Sea [21–24]. To its north, it is bounded by the Panyu Low Uplift, while the Yunli Low Uplift and the Yunxing Low Uplift bound it to the south. The western side is constrained by a northwest-trending basement fracture and magmatism zone, while the eastern side is flanked by the Dongsha Uplift (Figure 1a) [25–27].

The formation of the Baiyun Sag can be attributed to tensional action during the Late Cretaceous–Late Oligocene, which caused the continental lithosphere at the northern margin of the South China Sea to thin significantly towards the opening of the ocean. Simultaneously, extensional action increased towards the oceanic opening [28]. As a result, the Baiyun Sag developed precisely where the continental lithosphere was severely thinned and experienced strong extensional action during the Late Cretaceous–Late Oligocene, leading to the deposition of the Wenchang Formation, with a maximum thickness of 3400 m, and the Enping Formation, with a maximum thickness of 1500 m. These formations represent the two most important sets of hydrocarbon source rocks in this region [29–31]. The Nanhai Movement, which began around 32 million years ago during the Late Oligocene, facilitated large-scale marine intrusion into the northern land margin of the South China Sea, gradually developing a stable shelf-slope topography. During the period from 32 million years ago to 23.8 million years ago, the northern shelf-slope folding zone of the South China Sea developed relatively stable on the southern slope of the Baiyun Sag. The main body of the sag was situated in a shelf environment, and it deposited the Zhuhai Formation, which exhibits a maximum thickness of 1850 m (Figure 1c) [32–34].

2.2. Stratigraphy and Depositional Facies

The Cenozoic evolution of the Baiyun Sag can be divided into three distinct tectonic stages: the fault subsidence stage, the fault–sag transition stage, and the depression stage. These stages correspond to different sedimentary environments, namely terrestrial fluvial lake sedimentary environments during the Eocene–Early Oligocene, shallow marine shelf sedimentary environments during the Enping Formation, and land-slope deep-water sedimentary environments [35–37].

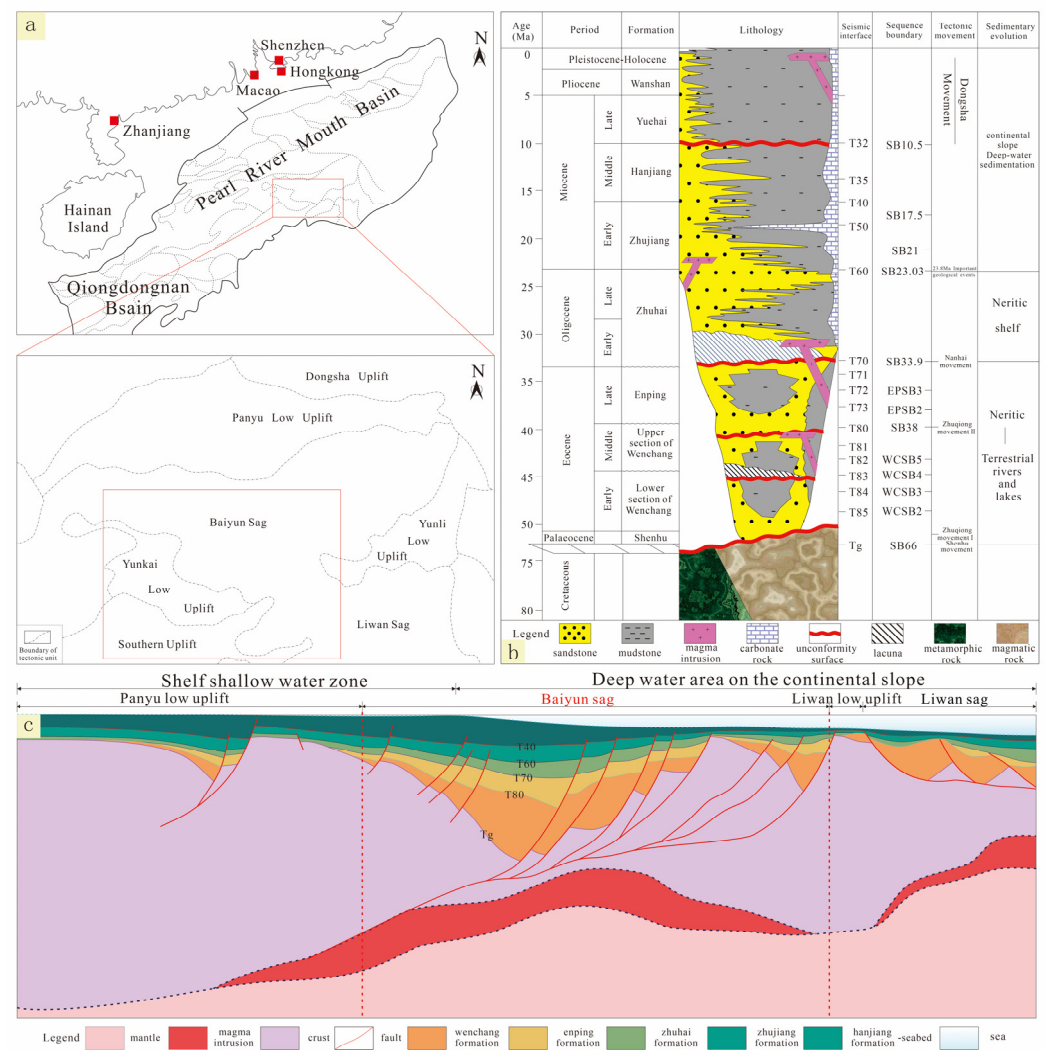


Figure 1. Tectonic position, stratigraphic development characteristics, and tectonic section of the Baiyun Sag: (a) location map of the study area; (b) integrated tectonic–sedimentary histogram of the deep-water area (according to [31] revised); and (c) the tectonic cross-section of the study area is a figure.

During the subsidence phase in the Eocene–Early Oligocene, the Wenchang Formation underwent river and lake phases. The lithology of the formation mainly consists of medium-thick grey–brown–light grey mudstone interbedded with medium-thin siltstone and clayey siltstone. Occasional coal seams and locally found igneous rocks, such as tuffs, basalts, and andesites, are also present [38–41]. The Enping Formation was subsequently filled by fluvial (braided river) deltaic–shallow marine sediments. In the middle and lower parts, the lithology of the formation is primarily medium-thick-bedded medium-coarse sandstone interbedded with medium-thin-bedded mudstone, while the upper part contains light grey mudstone interbedded with medium-thin-bedded sandstone.

During the Late Oligocene, the tectonic stage shifted to fracture transition, with the development of a large-scale shelf delta of the Zhuhai Group and shallow coastal marine fill. The lithology during this stage mainly comprises medium-thickness griststone with thin mudstone.

From the Miocene to the present, the Baiyun Sag experienced a period of argillaceous subsidence, primarily marked by the deposition of the Zhujiang Formation, Hanjiang Formation, Yuehai Formation, Wanshan Formation, and Pleistocene–Holocene deep-water fan and bathyal deep sea argillaceous deposits (Figure 1b) [42–44].

3. Materials and Methods

This study is based on data from 7 existing core holes in the southwest area of the Baiyun Depression. The research approach involves rock chip sampling, single-well burial thermal evolution history analysis, microscopic observation, statistical analysis of cast thin sections, electron microscope scanning for microscopic diagenesis phenomenon analysis, wavelet analysis, and the testing of carbon and oxygen isotopes and the physical properties of sandstone carbonate cement (Figure 2). In the laboratory, the rock samples were first washed, dried, and then crushed to 200 mesh. CO₂ was produced using the phosphoric acid method and the CO₂ gas obtained was analyzed using a Mat253 mass spectrometer to obtain the $\delta^{18}\text{O}$ and $\delta^{13}\text{C}$ values. Through these methods, the burial thermal history and diagenetic evolution characteristics of Paleogene sandstones in the southwest area of the Baiyun Sag were thoroughly investigated.

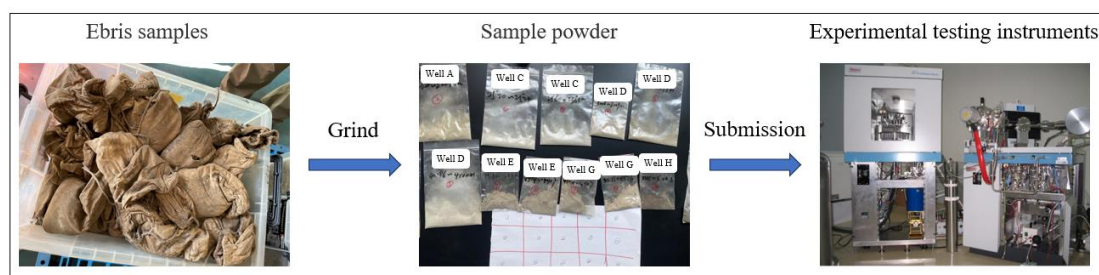


Figure 2. Carbon and oxygen isotope experimental process.

The main objectives of this study are to analyze the diagenetic characteristics of high-quality sandstone reservoirs in the Zhuhai Formation and Enping Formation and to examine the genesis characteristics, distribution rules, and controlling factors of favorable reservoirs. By comprehensively studying these aspects, the research aims to gain valuable insights into the diagenetic processes that have shaped the reservoirs' properties in this region, particularly identifying and understanding the favorable reservoirs with high potential for hydrocarbon accumulation.

4. Results

4.1. Petrology Characteristics

Based on the statistics of existing drilling data and analysis of 61 sets of thin-section data in the southwest area, it is evident that the Zhuhai Formation mainly comprises feldspathic quartz sandstone and feldspar sandstone, while the Enping Formation consists mainly of feldspathic quartz sandstone, feldspar sandstone, and lithic quartz sandstone (Figure 3).

The clastic particle composition of the Zhuhai Formation, on the whole, exhibits $Q_{77.96}F_{14.48}R_{7.56}$, with the quartz content ranging from 66% to 94% and an average value of 77.96%. The feldspar content varies between 1% to 24%, with an average value of 14.48%, while the rock debris content ranges from 2% to 18%, with an average value of 7.56%. In contrast, the clastic particle composition of the Enping Formation shows $Q_{72.17}F_{14.73}R_{13.10}$, with the quartz content ranging from 52% to 89% and an average value of 72.17%. The feldspar content ranges from 4% to 29%, with an average value of 14.73%, and the rock debris content ranges from 2% to 42%, with an average value of 13.10%.

4.2. Reservoir Physical Properties

Under the combined influence of sedimentary facies, lithology, grain size differences, and late diagenesis, the porosity of the Paleogene sandstones in the southwest of the Baiyun Sag exhibits significant variability, generally ranging from 5.2% to 28.9%, with an average of 18.3%. The frequency of different porosity distributions is between 7% and 29% (Figure 4a). As for permeability, the samples demonstrate a wide range from 0.1 to 1396.2 mD, with

an average permeability of 315 mD. Notably, 56% of the samples fall within the range of 100–1000 mD, and the distribution frequency of different permeability values is between 2.9% to 55.6% (Figure 4b).

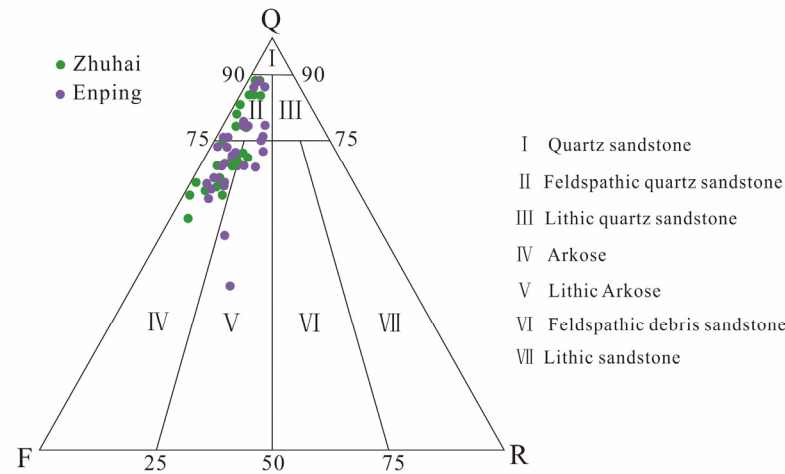


Figure 3. Sandstone type triangle diagram of the southwest Baiyun sag. (Classification scheme based on Yunfu Zeng, 1986 [45]).

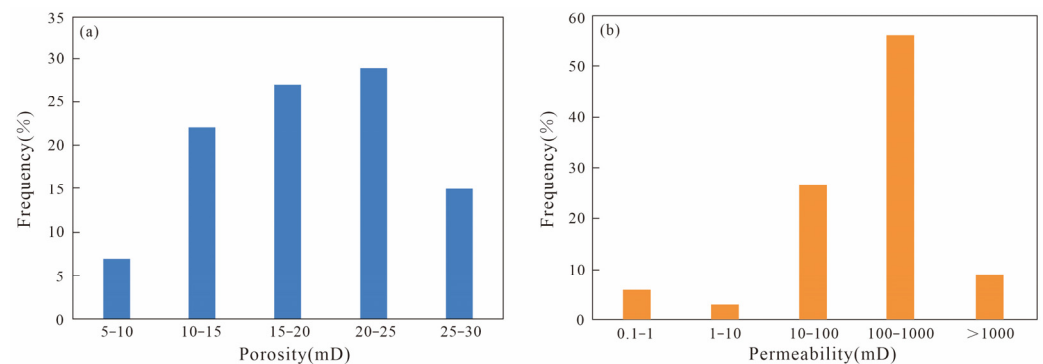


Figure 4. Physical properties of Paleocene sandstone reservoirs in the southwest of the Baiyun Sag: (a) porosity distribution frequency diagram and (b) permeability distribution frequency diagram.

The porosity and permeability intersections reveal a positive correlation between the porosity (x) and permeability (y) of the Paleogene sandstone reservoirs in the Baiyun Sag ($y = 51.12x - 635.27$, $R^2 = 0.6774$). This correlation indicates that the permeability of the sandstones is influenced by the associated pore space (Figure 5).

To study the longitudinal development characteristics of reservoir physical properties, Well A, located in the southwest Yunkai low uplift of the Baiyun Sag, serves as an example. Below the depth of 2550 m, the well exhibits mainly medium- and high-porosity ($\Phi \geq 15\%$) reservoirs, while the deeper section beyond 2550 m primarily consists of low-porosity and tight reservoirs. In the Zhuhai Formation, porosity increases with depth due to the occurrence of dissolution processes involving detrital mineral particles and carbonate cement. These processes lead to the formation of numerous intergranular pores and intragranular dissolution pores, resulting in an overall increase in pore volume. However, in the Enping Formation, porosity decreases with depth. The change range of permeability is considerable, and its vertical distribution characteristics align with those of porosity. Specifically, with increasing depth, the permeability of the Zhuhai Formation first increases and then decreases. In contrast, the porosity and permeability of both formations display gradual decreases with depth, according to Figure 6.

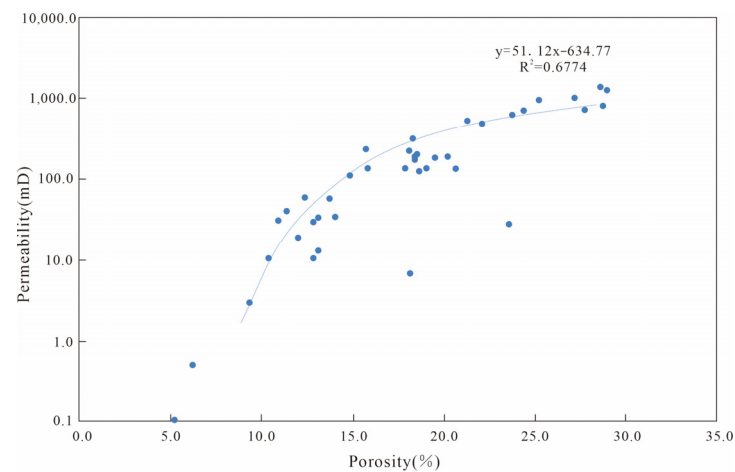


Figure 5. Relationship between the porosity and permeability of sandstone in the southwest deep-water area of the Baiyun sag (The blue dot represents the permeability input point corresponding to each porosity).

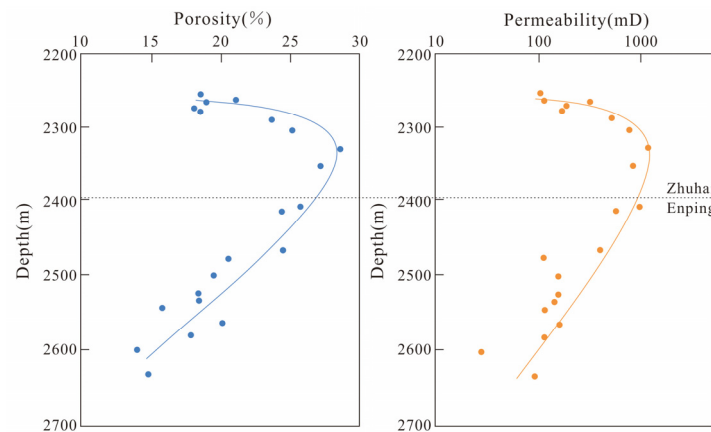


Figure 6. The relationship between the porosity, permeability, and depth of Well A in the Southwest Baiyun Sag (Blue dots represent the corresponding porosity of samples at different depths; Yellow dots represent the corresponding permeability of samples at different depths).

Common types of pores in sandstone reservoirs include intergranular dissolved pores, molded pores, intragranular dissolved pores, and intergranular pores, as well as microfractures in clay minerals [45]. In the Paleogene reservoir of the southwest Baiyun Sag, thin-section and scanning electron microscope analyses of samples from key exploration wells revealed that the pores are primarily dominated by secondary pores, with a smaller number of microcracks. Among the secondary pores, intergranular dissolved pores and mold pores are prominent (Figure 7a,b), along with intergranular pores and a minor number of intragranular dissolved pores (Figure 7c). Thin-section observations further reveal a considerable number of mold pores (Figure 7a), intragranular dissolved pores (Figure 7c), and intergranular dissolved pores (Figure 7b), along with a few developed microcracks.

Porosity plays a vital role in improving the physical properties of sandstone reservoirs, particularly when secondary dissolved pores are present. These secondary pores enhance reservoir connectivity to a certain extent and facilitate fluid flow through the interconnected pore network. Additionally, some of the pores are filled with various types of matrices and cement, such as mud, calcite, and dolomite (Figure 7d–f), which contribute to the overall complexity and heterogeneity of the reservoir system.

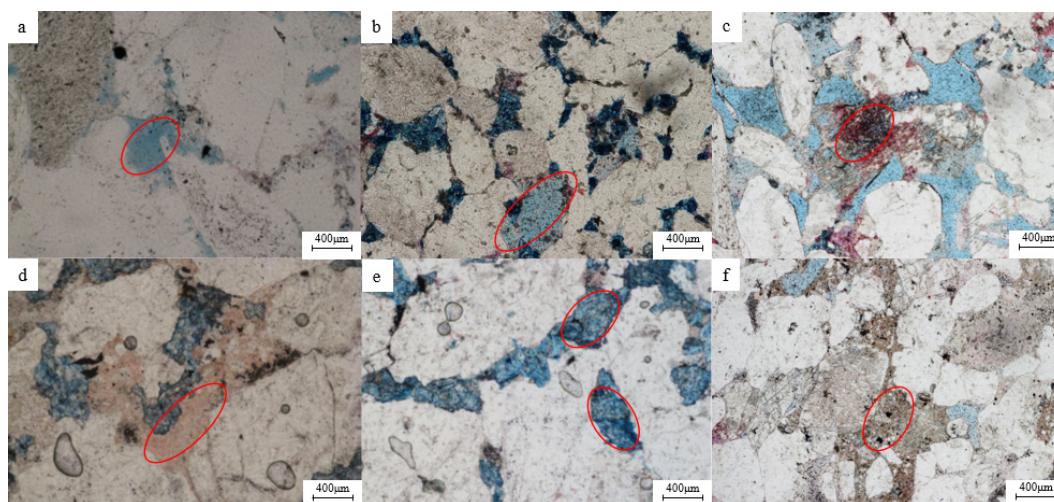


Figure 7. Microscopic photos of Paleogene reservoir pores in the Baiyun Sag. (a) Well B, 4150.0 m, Enping, intergranular dissolved pore; (b) Well C, 4098.3 m, Enping, the feldspar is completely dissolved to form a mold pore; (c) Well C, 3354.6 m, Enping, feldspar dissolves to form dissolution pores in feldspar grains; (d) Well D, 5109.0 m, Enping, the tuffaceous filled the intergranular pores and sericitization occurred; (e) Well D, 5109.0 m, Enping, ankerite filling intergranular; and (f) Well C, 3651.2 m, Enping, the mud is a mixed matrix filling and intergranular.

4.3. Wavelet Analysis

Due to the limited drilling data and incomplete lithological information in the study area, wavelet transform technology was employed to process the existing GR (gamma ray) logging data using Matlab2018. This approach enables us to better understand the changing patterns of the stratigraphic sequence and accurately identify the corresponding sequence interfaces. Different sequence frameworks play a crucial role in controlling the spatial distribution of each diagenetic effect and influencing the reservoir physical properties in the corresponding sequence units.

Taking Wells E and C in the study area as examples, the Zhuhai Formation–Enping Formation of the Baiyun Sag in the Pearl River Mouth Basin can be roughly divided into four third-order sequences (Figure 8). The analysis shows discernible changes in trend for the GR imaginary lines and shifts in lithological combinations during logging. The stratigraphic interfaces are identifiable as bright spots and superposition phenomena visible in the time–frequency chromatographic curves, and the wavelet coefficient curves demonstrate significant fluctuations. Through this approach, we gain valuable insights into the complex stratigraphic sequences and their influence on diagenetic processes, providing a basis for understanding the reservoir physical properties within the study area.

4.4. Seismic Facies Analysis

Seismic facies is the comprehensive response of sedimentary processes and sedimentary bodies in sedimentary areas to earthquakes, which can explain the relationship between source supply intensity and water body transformation and reflect the intensity of source transport and water body energy. Therefore, the indication of seismic facies can reflect the sedimentary environment at that time.

In response to the specific characteristics of multiple sedimentary types, complex tectonic processes, scarce and unevenly distributed drilling in the southwest of the Baiyun Depression, based on familiarity with the geological characteristics, stratigraphic sedimentary sequences, and distribution characteristics of the southwest of the Baiyun Depression, seismic facies analysis was conducted using three-dimensional data. The classification of seismic phase types is described and was classified based on the amplitude, frequency, and continuity characteristics of seismic events. A total of 11 types were identified during the research process (Table 1).

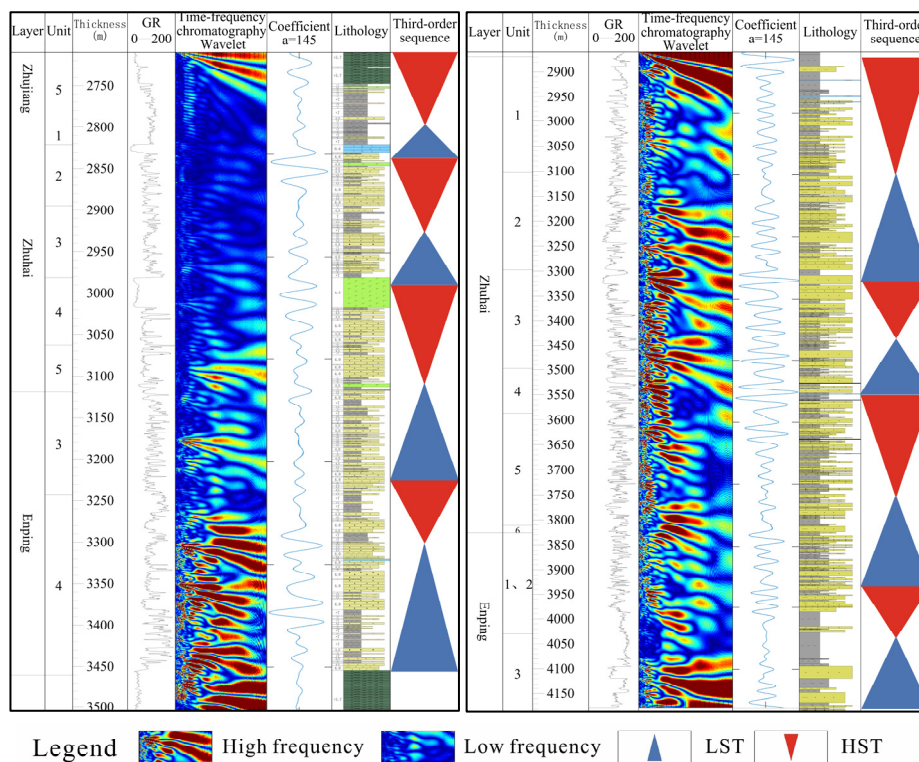
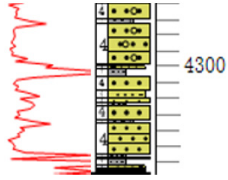
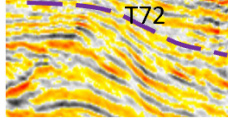
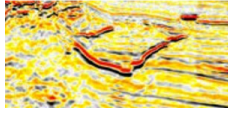


Figure 8. The sequence interface of the Enping–Zhuhai Formation in deep water are of the Baiyun Sag.

Table 1. Seismic facies, logging facies, and sedimentary facies types of sandstone types in the southwest of the Baiyun Depression.

Sedimentary Facies	Log Facies	Developmental Interval	Seismic Facies	Legend of Seismic Facies
Deep Lake—Sub Deep Lake		Enping–Zhuhai	Medium strong amplitude—medium–low frequency—continuous reflection	
Shore-shallow lake		Enping–Zhuhai	Medium amplitude high-frequency continuous parallel structure	
			Medium weak amplitude—medium frequency—more continuous reflection	
delta-plain		Enping–Zhuhai	Medium amplitude medium frequency weak continuity	
			Medium weak amplitude—medium–high frequency—medium continuous	

Table 1. Cont.

Sedimentary Facies	Log Facies	Developmental Interval	Seismic Facies	Legend of Seismic Facies
delta front		Enping–Zhuhai	S-shaped forward product reflection	
			Moderate strong amplitude difference continuous slightly forward product reflection	
incised valley		Enping	Strong amplitude top flat bottom convex, cutting relationship with surrounding strata	

4.5. Diagenesis Type of the Reservoirs

4.5.1. Compaction

The Zhuhai and Enping Formations in the study area exhibit complex types of compaction, with them displaying a wide range of planar distributions and depth spans. The main contact types observed are point, point-line, and line-point contacts. As the burial depth increases from shallow to deep, the contact type transitions from weak to strong compaction. In the southwest area, the geothermal gradient ranges from 4.5 to 5.3 °C/100 m. Under this high-temperature geothermal background, the Baiyun Sag reservoir experiences not only mechanical compaction but also strong thermal compaction. The overall trend for the line contacts indicates that the depth of the strong compaction boundary becomes shallower with an increasing geothermal gradient.

For instance, the burial depth of the Upper Enping Formation on the Yunkai Low Uplift is relatively shallow, approximately 2300–2800 m. As we go deeper, the contact type gradually changes from point to line-point contact. In the southwest fault zone, the Enping Formation is characterized by point-line contacts and line contacts, with a higher proportion of line contacts, while the Zhuhai Formation is predominantly composed of line-point contacts (Figure 9).

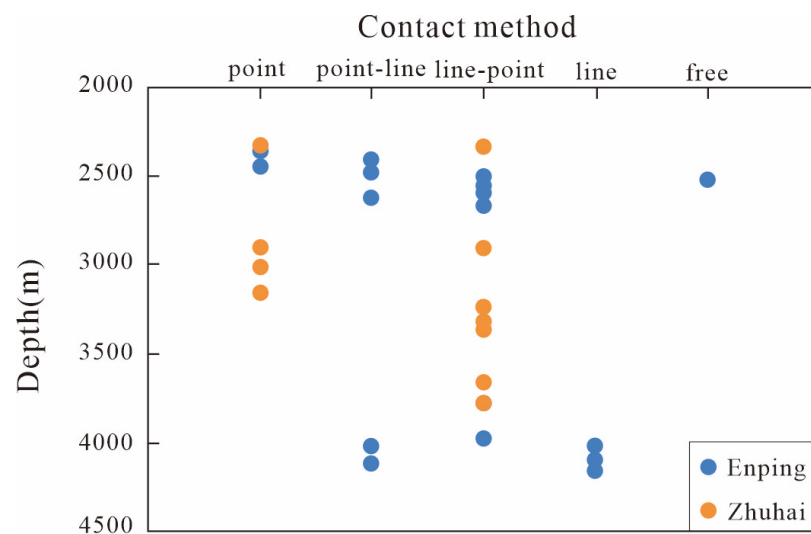


Figure 9. Longitudinal characteristics of the degree of compaction in the southwest of the Baiyun Sag.

Pressure solution plays a significant role in the compaction process, mainly occurring between quartz particles or between quartz particles and metamorphic quartzite debris. This pressure solution leads to particle contacts in the form of sutures (Figure 9a). The combination of mechanical compaction, thermal compaction, and pressure solution contributes to the complex compaction patterns observed in the Zhuhai and Enping Formations within the study area.

4.5.2. Cementation

In the southwest area of the Baiyun Sag, the cementation products in the sandstone reservoirs consist of a variety of minerals, including carbonate cements, quartz secondary enlargement, authigenic kaolinite, illite, chlorite, and pyrite.

Carbonate cements primarily include siderite, calcite, ferrocalcite, dolomite, and ankerite, with calcite, ferrocalcite, and ankerite being the most common types. Calcite is predominantly found filling intergranular pores or intergranular dissolution pores, appearing as bright crystals and hypocrystals, with debris particles dispersed within the crystalline calcite (Figure 10b). Sparry calcite or ferrocalcite occupies intergranular pores, and these sparry and hypocrySTALLINE calcite forms are typically developed during early diagenesis stages, with a low degree of compaction. Dolomite is mainly observed filling intergranular spaces in microcrystalline and sparry forms or as cemented and replacement grains (Figure 10c,d). The thin-section images show varying degrees of quartz secondary enlargement (Figure 10e,f). Additionally, microcrystalline quartz coexists with ankerite within the pores (Figure 10g). The symbiotic relationship between quartz secondary enlargement and ankerite indicates that quartz secondary enlargement is dependent on quartz grains, while ankerite forms later than quartz secondary enlargement.

Illite and kaolinite are the major types of clay minerals present in the reservoirs. Autochthonous kaolinite is primarily associated with the dissolution of feldspar, and it can often be observed filling intergranular or intragranular pores near the secondary pores formed due to the dissolution of feldspar grains (Figure 10h). Curled flake illite is distributed on the surface of the grains and fills the intergranular pores (Figure 10i). Pyrite appears in the form of microspheres and cubic aggregates, filling intergranular pores, and coexisting with illite and other minerals (Figure 10j). These cementation products and clay minerals play significant roles in the diagenetic evolution and physical properties of the sandstone reservoirs in the Baiyun Sag.

4.5.3. Dissolution

Dissolution plays a crucial role in enhancing the reservoir quality in the Baiyun Sag, with intergranular dissolved pores and intragranular dissolved pores being the primary pore types [46]. Acidic fluids act on soluble materials such as feldspars, debris, and tuffaceous matrices, leading to the formation of secondary pores (Figure 10k). The resulting pore network, comprising fractures and pores, significantly improves the physical properties of the reservoirs (Figure 10l). Autogenous quartz, ferrocalcite, or ankerite can fill into the dissolution pores (Figure 10b,h), and late cementation partially counteracts the pore-enhancing effects of dissolution. Deeper reservoirs tend to exhibit dissolution pores that are more likely to be associated with high compaction. In many instances, the dissolution pores occur between or within the point-line contact, line-point contact, and line-contact debris grains, suggesting that dissolution might have occurred after strong compaction. While various materials can undergo dissolution, feldspar appears to be the most commonly dissolved mineral.

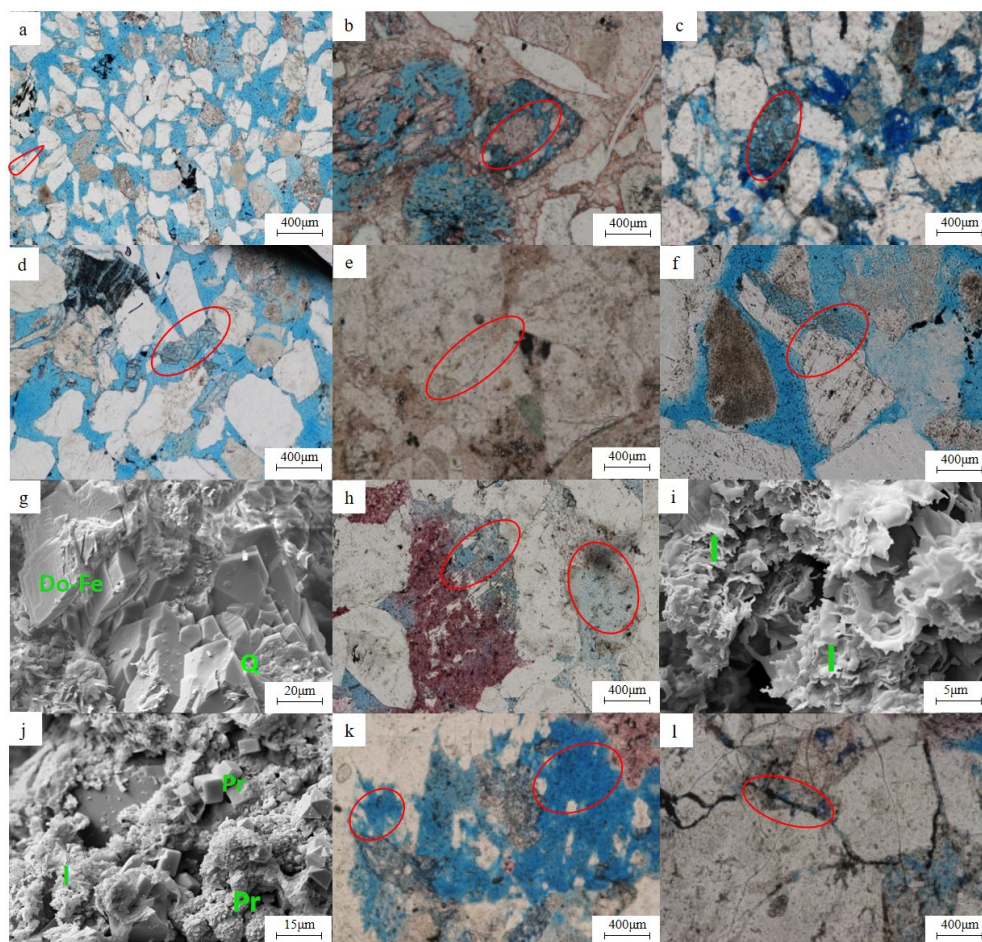


Figure 10. Diagenetic types of Paleogene sandstones in the southwestern Baiyun Sag: (a) Well F, 2327.5 m, Enping, pressure solubilisation, visible sutures between grains; (b) Well B, 3912.1 m, Zhuhai, calcite fills the pores of the grains; (c) Well D, 5116.0 m, Enping, ankerite is a fine and medium crystalline filling in the intergranular or cemented and metasomatism grains output; (d) Well F, 2437.0 m, Enping, ankerite is a fine and medium crystalline filling intergranular; (e) Well D, 5107.0 m, Enping, quartz secondary enlargement edge; (f) Well F, 2342.0 m, Enping, quartz secondary enlargement edge; (g) Well C, 4103.3 m, Enping, rhomboid ankerite and quartz secondary enlargement; (h) Well C, 3770.3 m, Zhuhai, dissolution of feldspar forms dissolved pores in the feldspar particles and kaolinite accumulates in situ; (i) Well F, 2479.1 m, Enping, the curled flake illite is distributed on the surface of the grains and filled with intergranular pores; (j) Well F, 2437.0 m, Enping, cubic, micro-spherical pyrite is distributed on the surface of the grains and fills the intergranular pores, and curly lamellar illite dissolution is seen; (k) Well D, 5109.0 m, Enping, intergranular dissolved pores and mold pores; (l) and Well D, 5116.0 m, Enping, grains fracture.

5. Discussion

5.1. Diagenetic Environment and Stages

Carbonate cementation is a significant diagenetic process in the Paleogene sandstone reservoirs of the southwest Baiyun Sag. To further analyze the impact of carbonate cementation on the reservoir physical properties and to identify the diagenetic environments and stages of the Paleogene sandstones in this area, carbon and oxygen stable isotope analyses were conducted on carbonate cements from 13 sandstone samples obtained from 6 wells in the Baiyun Sag (Table 2).

Table 2. Isotopic analyses of carbonate cementation in Paleocene sandstones of the Baiyun Sag.

Well	Depth/m	Formation	$\delta^{13}\text{C}/\text{PDB}$	$\delta^{18}\text{O}/\text{PDB}$	Z	Temperature/ $^{\circ}\text{C}$	Porosity/%	Permeability/%
A	2522	Enping	−10.430	−10.769	100.6	89.1	18.4	186.2
	2560	Enping	−18.319	−10.523	84.5	87.4	20.2	193.4
C	3005	Zhuhai	−2.915	−11.237	115.7	92.4	21.2	234.1
	4098	Enping	−2.711	−11.749	115.9	96.0	12.4	60.5
D	4025	Zhuhai	−5.015	−7.622	113.2	68.3		
	5082	Enping	−9.648	−11.540	101.8	94.5		
	5218	Enping	−11.75	−10.50	98.0	87.3		
E	3336	Enping	−5.413	−9.848	111.3	86.1		
	3450	Enping	−9.744	−10.543	102.1	87.6		
G	4381	Zhuhai	−6.138	−12.003	108.8	97.8	12.8	10.8
	4415	Zhuhai	−6.134	−12.048	108.7	98.2	13.7	58.1
H	4575	Enping	−5.333	−14.486	109.2	116.3		
	4606	Enping	−7.845	−14.267	104.1	114.6		

The test results reveal that the $\delta^{18}\text{O}$ values of the Paleogene sandstone samples in the southwest Baiyun Sag range from -14.486‰ to -7.622‰ and the $\delta^{13}\text{C}$ values range from -18.319‰ to -2.711‰ . Previous studies have demonstrated that as burial depth and formation temperature increase, pore water undergoes fluid–rock interactions, resulting in lower $\delta^{18}\text{O}$ values [47]. The measured $\delta^{18}\text{O}$ values of the Enping Formation in Well H are lower compared to the other five wells, indicating that the carbonate cements in the Enping Formation sandstones of Well H have been more significantly affected by burial heating. Additionally, the carbon isotopes in the carbonate cements have undergone exchange to some extent with carbon isotopes of organic acids released during early hydrocarbon generation in the source rocks [48].

The Z values of the carbonate cements in the Paleogene sandstones of the Baiyun Sag vary from 84.5 to 115.9 (Table 2). It can be seen that all wells are related to freshwater leaching. Wells A and E in the Yunkai Low Uplift, Well D in the Main Depression, and Well H in the Liwan Sag demonstrate a gradual decrease in Z value with increasing burial depth, indicating a trend towards the decreasing ambient salinity of carbonate cements in sandstone reservoirs. However, the diagenetic environments of Wells C and G, situated in the southwest fracture terrace zone, remain relatively unchanged.

The diagenetic temperatures of the Paleogene sandstones in the southwest Baiyun Sag span a wide range between 68.3 and 116.3 $^{\circ}\text{C}$, with the average temperature centered around 93.5 $^{\circ}\text{C}$ (Table 2). The carbonate cementation of Paleogene sandstones in this area primarily occurred during the early diagenetic stage B to the middle diagenetic stage A. Specifically, the carbonate cementation of sandstones in the upper part of the Zhuhai Formation in Well D predominantly took place during the early diagenetic stage B (65–85 $^{\circ}\text{C}$), while in other wells, it occurred during the middle diagenetic stage A (85–140 $^{\circ}\text{C}$).

Combining the reservoir physical properties from Wells A, C, and G, the temperature range for carbonate cementation in relatively shallowly buried strata is 89.1–92.4 $^{\circ}\text{C}$. These strata exhibit really high measured porosity and permeability, ranging from 18.4 to 21.2% porosity and 186.2 to 234.1 mD permeability. However, in strata with a burial depth exceeding 4500 m, the diagenesis temperature of the carbonate record is 96.0–98.2 $^{\circ}\text{C}$. As the burial depth and diagenesis temperature increase, the physical properties of the reservoirs significantly decrease, resulting in porosity of 12.4%–13.7% and permeability of 10.8–60.5 mD (Figure 11).

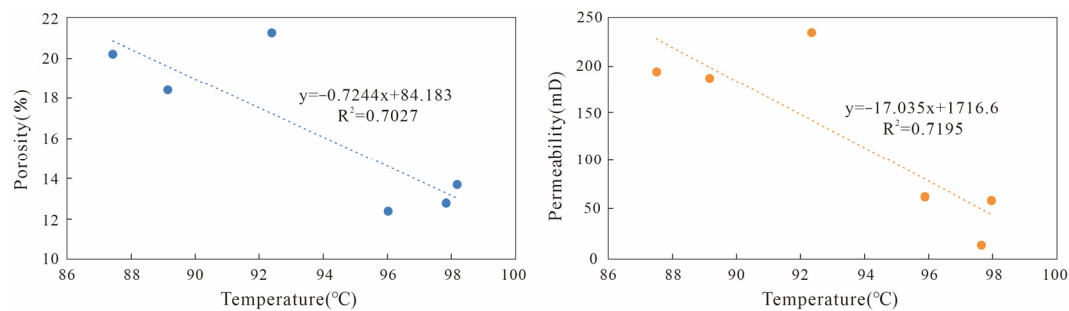


Figure 11. Paleocene porosity and permeability versus diagenetic temperature in the southwest of the Baiyun Sag. (Blue dots represent the corresponding porosity at different temperatures; Yellow dot represents the corresponding permeability at different temperatures)

Samples from the Zhuhai and Enping Formations mainly fall within the range associated with organic acid decarboxylation (Figure 12). The samples with carbon isotope distributions in the range of -9.848‰ to -3.236‰ indicate the influence of inorganic carbon sources and terrestrial debris from atmospheric precipitation during the Supergene period. On the other hand, the samples with distributions in the range of -18.319‰ to -10.430‰ display a significant negative carbon isotope bias, which is clearly related to hydrocarbon activities [49].

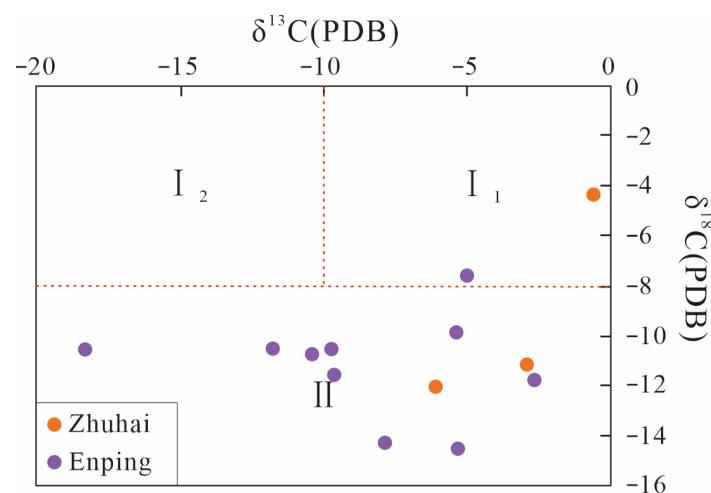


Figure 12. Carbon and oxygen isotope intersection diagram of carbonate cements in the Southwest Paleogene Baiyun Sag Sandstone.

Carbonate cementation of the Enping Formation sandstones took place in a deeper burial and higher paleotemperature environment. The relatively negatively biased carbon isotopes in these samples suggest increased activity of hydrocarbon-bearing fluids in the deep burial environment, creating favorable conditions for organic acid dissolution in this setting.

5.2. Diagenetic Sequence

Based on rock thin-section identification, diagenesis characterization, and analysis of diagenetic mineral interrelationships, the Paleogene sandstone reservoirs in the southwest of the Baiyun Sag have undergone various diagenetic sequences (Figure 13). These include shallow early mechanical compaction, early calcite precipitation and cementation, mid-term diagenetic fluid acidification, mid-late quartz secondary enlargement, and late ferric carbonate cement recrystallization filling. Different diagenetic effects have distinct impacts on reservoir porosity at different diagenetic stages. Compaction primarily occurs during the early diagenetic stage, leading to a reduction in reservoir porosity. Cementation

occurs predominantly in the early diagenetic stage B and the middle diagenetic stage, further decreasing reservoir porosity. Conversely, dissolution enhances reservoir porosity accordingly. This comprehensive analysis provides valuable insights into the diagenetic processes and their effects on the physical properties of the Paleogene sandstone reservoirs in the studied area.

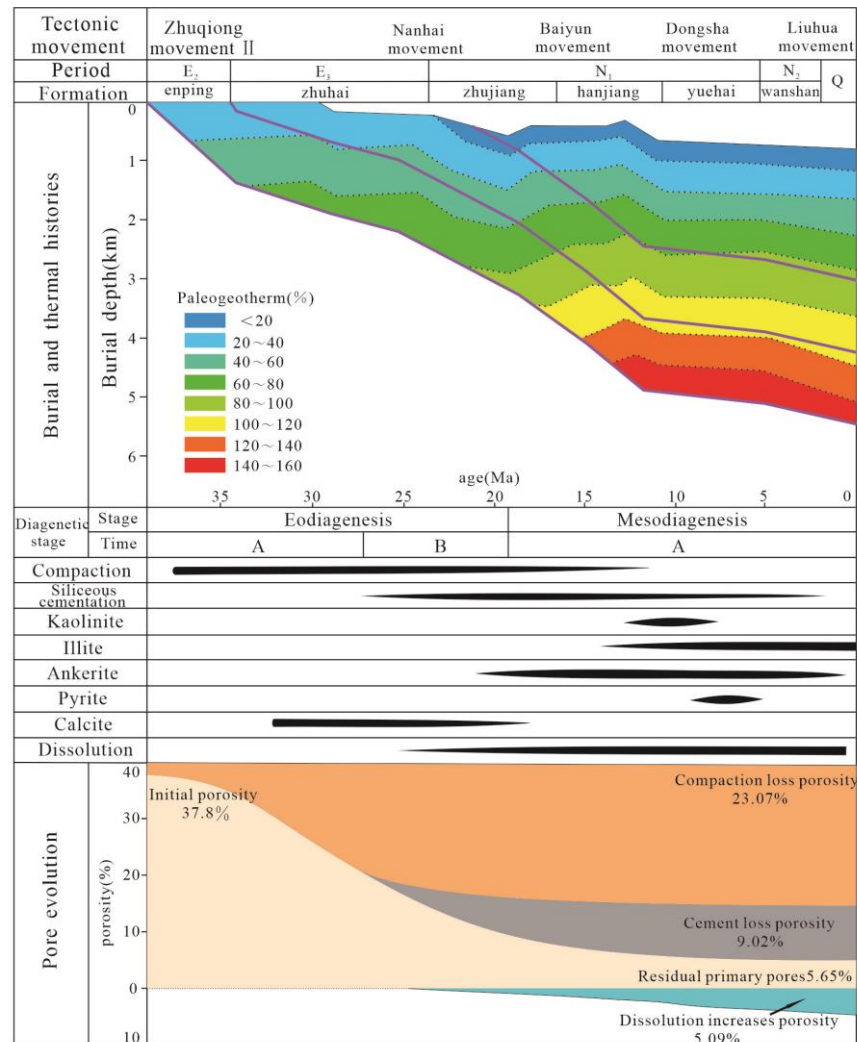


Figure 13. Pore evolution and stratigraphic burial history of the diagenetic sequence in the southwest of the Baiyun Sag.

5.3. Pore Evolution Characteristics

The evolution of pores in sandstone reservoirs is a result of changes in the diagenetic environment, such as paleotemperature and sedimentary fluids, and the transformation of various diagenetic processes. The content of the matrix and the composition of debris significantly influence compaction. Higher amounts of stabilizing minerals like quartz in debris lead to more stable physical properties during diagenesis, while increased depth generally results in a rapid decrease in reservoir porosity due to overall compaction.

Cementation also plays a crucial role in shaping the physical properties of the reservoirs, mainly through changes in the cementation content. Paleogene sandstones in the Baiyun Sag are primarily cemented by clay and carbonate minerals, which tend to decrease porosity as their content increases (Figure 13).

The pore evolution of sandstone reservoirs in the southwest of the Baiyun Sag is mainly influenced by diagenetic processes such as compaction, cementation, and dissolution. The average porosity lost due to compaction is 23.07%, while the average porosity lost due to

the cementation of carbonate and clay minerals is 9.02%. Compaction has a more significant impact on reducing porosity compared to cementation. On the other hand, the average porosity improvement resulting from diagenetic processes like feldspars, lithic grains, and the dissolution of minerals is 5.09% (Table 3; Figure 13). These findings highlight the complex interplay of the diagenetic factors shaping the physical properties of sandstone reservoirs in the Baiyun Sag.

Table 3. Quantitative analysis of the diagenetic porosity of Paleogene sandstone reservoirs in the Baiyun Sag.

Formation	Initial Porosity/%	Compaction Loss Porosity/%	Dissolution Increases Porosity/%	Cement Loss Porosity/%	Residual Primary Porosity/%
Zhuhai	36.91	24.03	5.56	5.64	7.11
Enping	38.69	22.11	4.63	12.39	13.0

5.4. The Impact of Diagenetic Evolution on Reservoirs

The diagenetic evolution of Paleogene sandstone reservoirs in the Baiyun Sag can be classified into three types based on data from core cast thin-section and scanning electron microscopy, taking into account the morphological types, structural features, and pore distribution characteristics of various diagenetic minerals (Figure 14).

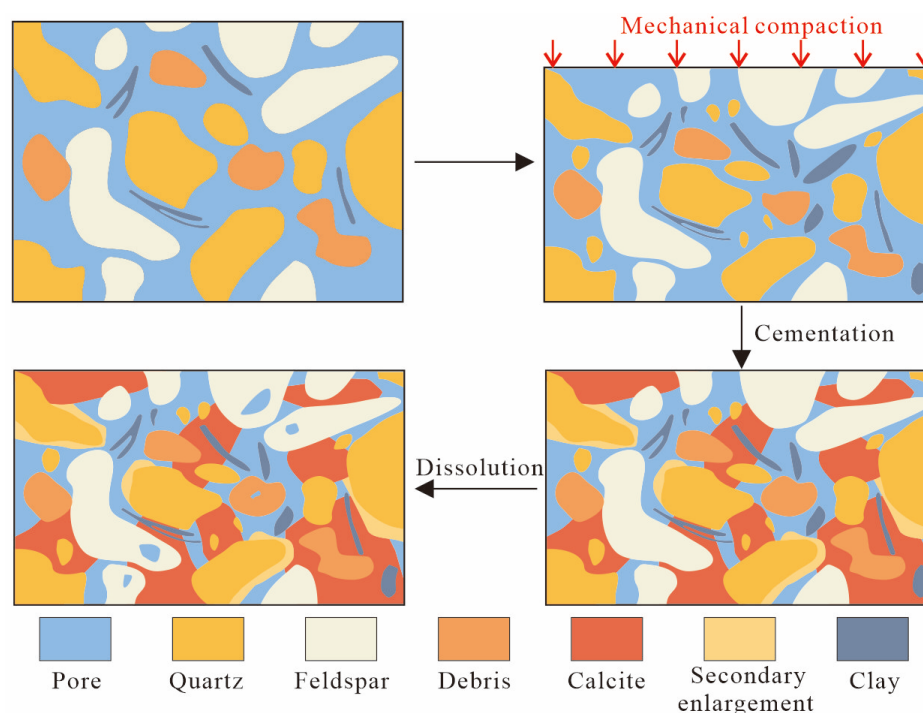


Figure 14. Diagenetic evolution of Paleogene sandstones in the southwestern Baiyun Sag.

- (1) **Mainly Mechanical Compaction:** This type is primarily observed in the Zhuhai Formation at burial depths exceeding 2300 m, with diagenesis temperatures ranging from 72 to 90 °C. In the early diagenetic stage, the sandstone grains are loose, and primary pores are well-preserved. However, as the burial depth increases, the grain arrangement becomes progressively tighter, and primary pores are filled with authigenic clay minerals, leading to the densification of the reservoir. Unstable clastic grains, such as feldspars, are prone to dissolution, and some rigid grains may fracture. This diagenetic evolution results in poor reservoir performance.

- (2) **Unstable Clastic Dissolution Dominant:** This type is mainly found in the Zhuhai Formation and the upper part of the Enping Formation, at burial depths of 2300 to 3500 m, with diagenesis temperatures ranging from 70 to 95 °C. Reservoirs with larger particle diameters, better sorting, and higher pore permeability are observed. There is less compaction, and primary pores are well-preserved. Intense dissolution enhances the physical properties of the reservoir, with loose sandstone grains having a higher content of matrix and plastic debris. The main rock-forming minerals, such as calcite and kaolinite, are associated with feldspar dissolution. However, they fill only a small proportion of the pores in the reservoir, with them having little effect on porosity and permeability.
- (3) **Dominated by Carbonate Rocks Cemented with Clay Minerals:** This type is more developed in the lower part of the Enping Formation, at burial depths exceeding 3500 m, with diagenesis temperatures ranging from 120 to 146 °C. The diagenetic evolution is mainly characterized by carbonate rocks cemented with clay minerals, with pore fills dominated by calcite, ferrocalcite, kaolinite, and illite. Secondary dissolution pores are minimal, with only a few remaining primary pores and feldspar dissolution pores as the main reservoir space. As most primary pores are filled by cement and the degree of dissolution is low, the storage space is limited, resulting in relatively poor pore permeability in reservoirs of this type of diagenetic evolution.

6. Conclusions

- (1) The Paleogene sandstones within the Baiyun Sag predominantly comprise feldspathic quartz sandstones and feldspathic sandstones. The reservoirs exhibit a predominance of secondary porosity, complemented by a minor presence of fractures. In the Zhuhai Formation and the upper segment of the Enping Formation reservoirs, intergranular dissolution pores dominate, followed by intragranular dissolution pores, contributing to higher permeability. Conversely, the lower segment of the Enping Formation reservoirs primarily exhibits intragranular dissolved pores, with relatively well-developed micropores resulting in lower permeability.
- (2) At greater depths, reservoir porosity exhibits a clear declining trend. Remarkably, a secondary pore development zone emerges at 2280–2350 m, characterized primarily by intergranular dissolution pores and intragranular dissolution pores. This unique zone is a consequence of the diverse impact of diagenetic processes on the reservoir physical properties.
- (3) Seismic signatures of the Zhuhai and Enping formations are classified into four third-order sequences. Carbonate cement in the upper Zhuhai Formation originated from a mixed-water diagenetic environment, while the lower Zhuhai Formation and Enping Formation sandstone reservoirs underwent freshwater diagenesis. The diagenetic temperatures ranged from 42.6 to 116.3 °C. Sandstones of the upper Zhuhai Formation correspond to Early Diagenesis Stage B, while the lower Zhuhai Formation and Enping Formation correspond to Middle Diagenesis Stage A.
- (4) In the deepwater area of the Baiyun Sag, sandstone reservoirs have undergone three main diagenetic evolution processes: compaction leading to a reduction in porosity of 23.07%, cementation leading to a reduction of 9.02%, and dissolution enhancing porosity leading to a reduction of 5.09%. The diagenetic evolution is characterized by mechanical compaction, carbonate cementation, and feldspar dissolution. Notably, feldspar dissolution contributes to the formation of high-quality reservoirs, making the sandstone in the upper part of the Enping Formation a conventional high-quality reservoir.

Author Contributions: Conceptualization, Q.F. and G.Z.; methodology, Q.F.; software, G.P.; validation, G.Z., Q.F. and X.W.; formal analysis, L.Z.; investigation, X.X.; resources, G.P.; data curation, X.X. and Z.Z.; writing—original draft preparation, G.Z.; writing—review and editing, G.Z.; visualization,

Q.F.; supervision, G.P.; project administration, G.P. All authors have read and agreed to the published version of the manuscript.

Funding: This research received no external funding.

Data Availability Statement: Due to the nature of this research, participants of this study did not agree for their data to be shared publicly.

Acknowledgments: We would like to thank the China National Offshore Oil Corporation (CNOOC) for the provision of geological data and borehole samples. The careful review of the manuscript and the constructive suggestions given by anonymous reviewers are greatly appreciated.

Conflicts of Interest: The authors declare that there is no conflict of interest.

References

1. Zhang, G.C.; Yang, H.Z.; Chen, Y.; Ji, M.; Wang, K.; Yang, D.S.; Han, Y.X.; Sun, Y. The Baiyun Sag: A giant rich gas-generation sag in the deepwater area of the Pearl River Mouth Basin. *Nat. Gas Ind.* **2014**, *34*, 11–25.
2. Han, J.; Xu, G.; Li, Y.; Zhuo, H. Evolutionary history and controlling factors of the shelf breaks in the Pearl River Mouth Basin, northern South China Sea. *Mar. Pet. Geol.* **2016**, *77*, 179–189. [[CrossRef](#)]
3. Xiao, X.M.; Li, N.X.; Gan, H.J.; Jin, Y.B.; Tian, H.; Huang, B.J.; Tang, Y.C. Tracing of deeply-buried source rock: A case study of the WC9-2 petroleum pool in the Pearl River Mouth Basin, South China Sea. *Mar. Pet. Geol.* **2009**, *26*, 1365–1378. [[CrossRef](#)]
4. Yu, X.; Wang, J.; Liang, J.; Li, S.; Zeng, X.; Li, W. Depositional characteristics and accumulation model of gas hydrates in northern South China Sea. *Mar. Pet. Geol.* **2014**, *56*, 74–86. [[CrossRef](#)]
5. Wang, W.; Yang, X.; Bidgoli, T.S.; Ye, J. Detrital zircon geochronology reveals source-to-sink relationships in the Pearl River Mouth Basin, China. *Sediment. Geol.* **2019**, *388*, 81–98. [[CrossRef](#)]
6. Jiang, Z.; Du, H.; Li, Y.; Zhang, Y.; Huang, Y. Simulation of Gas Generation from the Paleogene Enping Formation in the Baiyun Sag in the Deepwater Area of the Pearl River Mouth Basin, the South China Sea. *Energy Fuels* **2015**, *29*, 577–586. [[CrossRef](#)]
7. Shi, C.; Long, Z.; Zhu, J.; Jiang, Z.; Huang, Y. Element geochemistry of the Enping Formation in the Baiyun Sag of Pearl River Mouth Basin and their environmental implications. *Mar. Geol. Quat. Geol.* **2020**, *40*, 79–86.
8. Zeng, Z.; Zhu, H.; Mei, L.; Du, J.; Zeng, H.; Xu, X.; Dong, X. Multilevel source-to-sink (S2S) subdivision and application of an ancient uplift system in South China Sea: Implications for further hydrocarbon exploration. *J. Pet. Sci. Eng.* **2019**, *181*, 106220. [[CrossRef](#)]
9. Ma, B.; Gao, J.; Eriksson, K.A.; Zhu, H.; Liu, Q.; Ping, X.; Zhang, Y. Diagenetic alterations in Eocene, deeply buried volcanoclastic sandstones with implications for reservoir quality in the Huizhou depression, Pearl River Mouth Basin, China. *Aapg Bull.* **2023**, *107*, 929–955. [[CrossRef](#)]
10. Li, C.; Luo, J.L.; Hu, H.Y.; Chen, S.; Wang, D.; Liu, B.; Ma, Y.; Chen, L.; Li, X. Thermodynamic Impact on Deepwater Sandstone Diagenetic Evolution of Zhuhai Formation in Baiyun Sag, Pearl River Mouth Basin. *Earth Sci.* **2019**, *44*, 572–587.
11. Zhuo, H.; Wang, Y.; Sun, Z.; Wang, Y.; Xu, Q.; Hou, P.; Wang, X.; Zhao, Z.; Zhou, W.; Xu, S. Along-strike variability in shelf-margin morphology and accretion pattern: An example from the northern margin of the South China Sea. *Basin Res.* **2019**, *31*, 431–460. [[CrossRef](#)]
12. Zeng, Z.; Zhu, H.; Yang, X.; Zhang, G.; Zeng, H. Three-dimensional imaging of Miocene volcanic effusive and conduit facies: Implications for the magmatism and seafloor spreading of the South China Sea. *Mar. Pet. Geol.* **2019**, *109*, 193–207. [[CrossRef](#)]
13. Gao, N.; Lin, C.; Eriksson, K.; Zhang, Z.; Gao, D.; Zhang, B.; Shu, L.; Wei, A. Sequence architecture and depositional evolution of Eocene to Oligocene, synrift to early postrift strata in the Baiyun Sag, South China Sea. *Interpret.-A J. Subsurf. Character.* **2019**, *7*, T309–T329. [[CrossRef](#)]
14. Ma, M.; Chen, G.J.; Li, C. Quantitative analysis of porosity evolution and formation mechanism of good reservoir in Enping Formation, Baiyun Sag, Pearl River Mouth Basin. *Nat. Gas Geosci.* **2017**, *28*, 1515–1526.
15. Peng, J.W.; Pang, X.Q.; Peng, H.J.; Ma, X.X.; Shi, H.S.; Zhao, Z.F.; Xiao, S.; Zhu, J.Z. Geochemistry, origin, and accumulation of petroleum in the Eocene Wenchang Formation reservoirs in Pearl River Mouth Basin, South China Sea: A case study of HZ25-7 oil field. *Mar. Pet. Geol.* **2017**, *80*, 154–170. [[CrossRef](#)]
16. Gong, C.; Wang, Y.; Zheng, R.; Hernández-Molina, F.J.; Li, Y.; Stow, D.; Xu, Q.; Brackenridge, R.E. Middle Miocene reworked turbidites in the Baiyun Sag of the Pearl River Mouth Basin, northern South China Sea margin: Processes, genesis, and implications. *J. Asian Earth Sci.* **2016**, *128*, 116–129. [[CrossRef](#)]
17. Wang, D.F.; Luo, J.L.; Chen, S.H.; Haiyan, H.U.; Yongkun, M.A.; Chi, L.I. Carbonate Cementation and Origin Analysis of Deep Sandstone Reservoirs in the Baiyun Sag, Pearl River Mouth Basin. *Acta Geol. Sin.* **2017**, *91*, 2079–2090.
18. Xu, S.H.; Wang, Y.M.; Xu, G.Q.; Zeng, G.D.; Guo, W.; Gong, C.L.; Cai, C.E.; Tang, W.; Zhuo, H.T.; Wan, H.Q. Linking shelf delta to deep-marine deposition in reservoir dispersal of the upper Oligocene strata in the Baiyun Sag, the northern South China Sea. *Aust. J. Earth Sci.* **2015**, *62*, 365–382.
19. Wen, J.; Zhao, J.; Li, J.; Er, C. Characteristics of Mid-Deep Paleogene Sandstone Reservoirs in Baiyun Sag and Controlling Effect of Dissolution on High-Quality Reservoirs. *Spec. Oil Gas Reserv.* **2022**, *29*, 47–55.

20. Wu, Y.; Ding, W.; Clift, P.D.; Li, J.; Yin, S.; Fang, Y.; Ding, H. Sedimentary budget of the Northwest Sub-basin, South China Sea: Controlling factors and geological implications. *Int. Geol. Rev.* **2020**, *62*, 970–987. [[CrossRef](#)]
21. Yang, L.; Ren, J.; McIntosh, K.; Pang, X.; Lei, C.; Zhao, Y. The structure and evolution of deepwater basins in the distal margin of the northern South China Sea and their implications for the formation of the continental margin. *Mar. Pet. Geol.* **2018**, *92*, 234–254. [[CrossRef](#)]
22. Clift, P.D.; Brune, S.; Quinteros, J. Climate changes control offshore crustal structure at South China Sea continental margin. *Earth Planet. Sci. Lett.* **2015**, *420*, 66–72. [[CrossRef](#)]
23. Ji, M.; Yang, H.; Zeng, Q.; Zhao, Z.; Wang, L.; Sun, Y. Structural analysis and its petroleum significance of detachment faults in Baiyun Sag, Pearl River Mouth Basin. *Nat. Gas Geosci.* **2017**, *28*, 1506–1514.
24. Zhou, Z.; Mei, L.; Liu, J.; Zheng, J.; Chen, L.; Hao, S. Continentward-dipping detachment fault system and asymmetric rift structure of the Baiyun Sag, northern South China Sea. *Tectonophysics* **2018**, *726*, 121–136. [[CrossRef](#)]
25. Longtao, S.U.N.; Di, Z.; Changmin, C.; Wenhuan, Z.; Zhen, S.U.N. Fault structure and evolution of Baiyun Sag in Zhujiang River Mouth Basin. *J. Trop. Oceanogr.* **2008**, *27*, 25–31.
26. Pang, X.; Zheng, J.; Ren, J.; Wang, F.; Yan, H.; Sun, H.; Liu, B. Structural Evolution and Magmatism of Fault Depression in Baiyun Sag, Northern Margin of South China Sea. *Earth Sci.* **2022**, *47*, 2303–2316.
27. Zhou, W.; Zhuo, H.; Wang, Y.; Xu, Q.; Li, D. Post-rift submarine volcanic complexes and fault activities in the Baiyun Sag, Pearl River Mouth Basin: New insights into the breakup sequence of the northern South China Sea. *Mar. Geol.* **2020**, *430*, 106338. [[CrossRef](#)]
28. Wang, W.; Zeng, Z.; Yang, X.; Bidgoli, T. Exploring the roles of sediment provenance and igneous activity on the development of synrift lacustrine source rocks, Pearl River Mouth Basin, northern South China Sea. *Mar. Petroleum Geol.* **2023**, *147*, 105990. [[CrossRef](#)]
29. Ye, Q.; Mei, L.; Shi, H.; Shu, Y.; Camanni, G.; Wu, J. A low-angle normal fault and basement structures within the Enping Sag, Pearl River Mouth Basin: Insights into late Mesozoic to early Cenozoic tectonic evolution of the South China Sea area. *Tectonophysics* **2018**, *731*, 1–16. [[CrossRef](#)]
30. Ge, J.W.; Zhu, X.M.; Zhang, X.T.; Jones, B.G.; Yu, F.S.; Niu, Z.C.; Li, M. Tectono-stratigraphic evolution and hydrocarbon exploration in the Eocene Southern Lufeng Depression, Pearl River Mouth Basin, South China Sea. *Aust. J. Earth Sci.* **2017**, *64*, 931–956. [[CrossRef](#)]
31. Pang, X.; Ren, J.; Zheng, J.; Liu, J.; Yu, P.; Liu, B. Petroleum geology controlled by extensive detachment thinning of continental margin crust: A case study of Baiyun sag in the deep-water area of northern South China Sea. *Pet. Explor. Dev.* **2018**, *45*, 29–42. [[CrossRef](#)]
32. Cheng, P.; Tian, H.; Huang, B.J.; Wilkins, R.W.T.; Xiao, X.M. Tracing early-charged oils and exploration directions for the Wenchang A sag, western Pearl River Mouth Basin, offshore South China Sea. *Org. Geochem.* **2013**, *61*, 15–26. [[CrossRef](#)]
33. Robison, C.R.; Elrod, L.W.; Bissada, K.K. Petroleum generation, migration, and entrapment in the Zhu 1 depression, Pearl River Mouth basin, South China Sea. *Int. J. Coal Geol.* **1998**, *37*, 155–178. [[CrossRef](#)]
34. Wu, X.; Zhou, D.; Pang, X.; Hao, H.; Shen, J. Geophysical Field and Deep Structures of Baiyun Sag, Zhujiang River Mouth Basin. *J. Trop. Oceanogr.* **2005**, *24*, 62–69.
35. Zeng, Z.; Zhu, H.; Yang, X.; Zeng, H.; Zhang, G. Multistage progradational clinoform-set characterisation and evolution analysis of the Early Oligocene in the Baiyun Sag, Pearl River Mouth Basin, South China Sea. *Mar. Pet. Geol.* **2020**, *112*, 104048. [[CrossRef](#)]
36. Kong, L.; Chen, H.; Ping, H.; Zhai, P.; Liu, Y.; Zhu, J. Formation pressure modeling in the Baiyun Sag, northern South China Sea: Implications for petroleum exploration in deep-water areas. *Mar. Pet. Geol.* **2018**, *97*, 154–168. [[CrossRef](#)]
37. Tian, B.; Zheng, Y.; Zhao, J. Sedimentary facies and evolution of Oligocene Zhuhai Formation in Baiyun Sag, South China Sea. *Fault Block Oil Gas Field* **2022**, *29*, 800–806,836.
38. Zeng, Z.; Zhu, H.; Yang, X.; Zeng, H.; Xia, C.; Chen, Y. Using seismic geomorphology and detrital zircon geochronology to constrain provenance evolution and its response of Paleogene Enping Formation in the Baiyun Sag, Pearl River Mouth Basin, South China sea: Implications for paleo-Pearl River drainage evolution. *J. Pet. Sci. Eng.* **2019**, *177*, 663–680.
39. He, D.; Hou, D.; Chen, T. Geochemical characteristics and analysis of crude-oil source in the deep-water area of the Baiyun Sag, South China Sea. *Russ. Geol. Geophys.* **2018**, *59*, 499–511. [[CrossRef](#)]
40. Guo, W.; Xu, G.; Chen, Z.; Li, X.; Xiang, X.; Liu, D. Sedimentary filling characteristics and evolution of the Paleogene Wenchang Formation in Baiyun main sag, Pearl River Mouth Basin. *J. Palaeogeogr.* **2022**, *24*, 112–128.
41. Guo, W.; Xu, G.; Liu, B.; Xiang, X.; Liu, D.; Zhang, B. Structure-Sedimentary Response Relationship of Wenchang Formation in Baiyun Sag, Pearl River Mouth Basin. *Earth Sci.* **2022**, *47*, 2433–2453.
42. He, D.; Hou, D.; Zhang, P.; Harris, M.; Mi, J.; Chen, T.; Li, J. Reservoir characteristics in the LW3-1 structure in the deepwater area of the Baiyun sag, South China Sea. *Arab. J. Geosci.* **2016**, *9*, 251. [[CrossRef](#)]
43. Li, Y.; Zheng, R.; Yang, B.; Zhu, G.; Hu, X. Provenance and Its Geological Implications of Miocene Zhujiang Formation in Baiyun Sag, Pearl River Mouth Basin. *Geol. Rev.* **2013**, *59*, 41–51.
44. Yuanli, H.O.U.; Lei, S.H.A.O.; Peijun, Q.I.A.O. Provenance of the Eocene-Miocene sediments in the Baiyun Sag, Pearl River Mouth Basin. *Mar. Geol. Quat. Geol.* **2020**, *40*, 19–28.
45. Zeng, Y.; Xia, W. *Sedimentary Petrology*; Gelogy Press: Beijing, China, 1986.

46. Gan, H.J.; Tian, H.; Huang, B.J.; Wilkins, R.W.T.; Tang, Y.C.; Xiao, X.M. Generation and accumulation of oil and condensates in the Wenchang A Sag, western Pearl River Mouth Basin, South China Sea. *Geofluids* **2009**, *9*, 275–286. [[CrossRef](#)]
47. Fisher, J.B.; Boles, J.R. Water Rock Interaction in tertiary sandstones, San-Joaquin Basin, California, USA-Diagenetic controls on water composition. *Chem. Geol.* **1990**, *82*, 83–101. [[CrossRef](#)]
48. Keith, M.L.; Weber, J.N. Systematic Relationships between Carbon and Oxygen Isotopes in Carbonates Deposited by Modern Corals and Algae. *Science* **1965**, *150*, 498–501. [[CrossRef](#)] [[PubMed](#)]
49. Curtis, C.D. Possible Links between Sandstone Diagenesis and Depth-Related Geochemical Reactions Occurring in Enclosing Mudstones. *J. Geol. Soc.* **1978**, *135*, 107–117. [[CrossRef](#)]

Disclaimer/Publisher’s Note: The statements, opinions and data contained in all publications are solely those of the individual author(s) and contributor(s) and not of MDPI and/or the editor(s). MDPI and/or the editor(s) disclaim responsibility for any injury to people or property resulting from any ideas, methods, instructions or products referred to in the content.